HHS Public Access

Author manuscript

Nat Immunol. Author manuscript; available in PMC 2012 December 27.

Published in final edited form as:

Nat Immunol. ; 12(10): 975–983. doi:10.1038/ni.2087.

The anti-viral factor APOBEC3G enhances natural killer cell recognition of HIV-infected primary T cells

Jason M. Norman[1], **Michael Mashiba**[2], **Lucy A McNamara**[1,3], **Adewunmi Onafuwa-Nuga**[4], **Estelle Chiari-Fort**[4], **Wenwen Shen**[4], and **Kathleen L. Collins**[1,2,4,*]

[1]Deparment of Microbiology and Immunology, University of Michigan, Ann Arbor, MI 48109

[2]Graduate Program in Immunology, University of Michigan, Ann Arbor, MI 48109

[3]Department of Epidemiology, University of Michigan, Ann Arbor, MI 48109

[4]Department of Internal Medicine, University of Michigan, Ann Arbor, MI 48109

Abstract

APOBEC3G (A3G) is an intrinsic antiviral factor that inhibits HIV replication by deaminating cytidine residues to uridine. This causes G-to-A hypermutation in the opposite strand and results in viral inactivation. HIV counteracts A3G through the activity of viral infectivity factor (Vif), which promotes A3G degradation. We report that viral protein R (Vpr), which interacts with a uracil glycosylase, also counteracts A3G by reducing uridine incorporation. However, this process results in activation of the DNA damage response pathway and expression of NK cell activating ligands. Our results reveal that pathogen-induced cytidine deamination and the DNA damage response to viral-mediated repair of uridine incorporation enhance recognition of HIV-infected cells by NK cells.

Following exposure to HIV, the acute phase of infection is characterized by high viral loads, which are counteracted by a rapid immune response[1]. The first line of defense against viral infections is the innate immune system, which uses pattern recognition receptors to detect pathogen associated molecular patterns. This response leads to cytokine secretion, which increases the expression of innate immune factors such as APOBEC3G (A3G) that limit viral replication and spread[2].

A3G is a member of a family of cytidine deaminases known as apolipoprotein B editing complex (APOBEC) proteins. In addition to inhibiting HIV, members of the APOBEC3 family inhibit DNA viruses and potentially harmful retrotransposition[3]. The mechanism by which A3G inhibits HIV replication is twofold. A3G is packaged into HIV particles and

*Corresponding author: Phone: 734-615-1320, Fax: 734-615-5252, klcollin@umich.edu.

Author Contribution

J.M.N. and K.L.C. designed the experiments and prepared the manuscript. J.M.N., M.M., L.A.M., A.O.N. W.S. and E.C.F. performed experiments. All authors read and edited the manuscript.

COMPETING FINANCIAL INTERESTS

The authors declare no competing financial interests

deaminates cytosine residues to uracils in exposed stretches of viral ssDNA during cDNA synthesis[4]. This editing leads to G to A hypermutation on the opposite strand, which inactivates the virus. A3G also inhibits the translocation of reverse transcriptase along template RNA, disrupting cDNA synthesis[5]. The importance of A3G in HIV disease pathogenesis is highlighted by the fact that genetic variation at the A3G locus predicts disease progression in HIV-infected people[6].

The viral infectivity factor (Vif) from HIV-1 counteracts A3G by targeting it for proteasomal degradation, thus reducing the amount of A3G incorporated into virus particles[7]. However, the action of Vif is not absolute and hypermutated viral genomes have been isolated from individuals harboring full-length HIV-1[8]. These sub-lethal mutations may influence HIV-1 evolution and promote the acquisition of drug resistance and immune evasion[9].

HIV-1-specific $CD8^+$ cytotoxic T lymphocytes (CTLs) decrease viremia during acute and chronic stages of the disease[10] but do not prevent the development of AIDS in most infected people. The HIV-1 Nef protein may limit the effectiveness of CTLs by downmodulating surface major histocompatibility complex class I (MHC-I) expression[11, 12]. However, MHC-I inhibits the lytic activity of natural killer (NK) cells and thus MHC-I downmodulation by Nef may increase susceptibility to NK cells.

Studies of NK cell inhibitory receptor allelic frequencies have provided strong evidence for a role of NK cells in limiting HIV infection. For instance, HIV-infected individuals expressing the NK cell inhibitory receptor KIR3DL1 and its cognate ligand, HLA-Bw4, progress to AIDS at a slower rate than individuals without this allelic combination[13]. This delayed progression likely results from a decrease in the activation threshold in the absence of inhibitory signals via HLA-Bw4, which is targeted by Nef in HIV infected individuals[14]. In addition, resistance to HIV-1 among sex workers is associated with a higher incidence of inhibitory *KIR* genes that lack their cognate inhibitory *HLA* ligand, which could lower the threshold for NK cell activation[15].

NK cell activating signals also influence the progression of HIV disease. Infected individuals who encode the NK cell activating receptor KIR3DS1 and HLA-Bw4-80Ile progress more slowly to AIDS[16], due to increased KIR3DS1 expression by $HLA\text{-}Bw4^+$ individuals[17]. Ligands detected by the NKG2D NK cell activating receptor also stimulate NK cell recognition. These ligands represent a diverse family of proteins commonly upregulated in viral infection[18] and can affect NK cell recognition in HIV infected people[19]. In sum, these studies provide strong evidence that NK cells influence HIV disease progression and that strategies aimed at enhancing NK cell activity may benefit HIV-infected people.

Recent reports have linked NKG2D activating ligand expression to viral protein R (Vpr)[20]. Known cellular targets bound by Vpr are DNA repair proteins, including the uracil DNA glycosylases UNG2 and SMUG1 [21, 22]. However, the role of these DNA repair proteins in the normal functioning of Vpr and their potential role in HIV disease pathogenesis is unknown.

Here, we examined the effect of A3G, Vif and Vpr on recognition of HIV-infected cells by NK cells. These studies uncover a role for A3G in alerting NK cells to the presence of viral pathogens and reveal the way HIV evades this response. Specifically, we provide evidence that pathogen-induced cytidine deamination and the DNA damage response to viral-mediated repair of uridine incorporation act as intrinsic antiviral responses by upregulating NK cell activating ligand expression and increasing the sensitivity of HIV infected cells to NK cell lysis.

Results

HIV accessory proteins alter expression of NKG2D ligands

To better understand the factors that influence NK cell recognition of HIV-infected cells, we used a recombinant human NKG2D-Fc fusion protein to directly measure protein expression of NKG2D ligands on primary T cells. Infection with HIVs that encoded all of the viral accessory proteins (Nef, Vif, Vpu and Vpr, Fig. 1a) resulted in about 3-fold more NKG2D ligand expression in infected cells than in mock-infected cells (Fig. 1b). This result was consistently observed in nine independent donors with upregulation varying from about 1.5 to 5 fold (Fig. 1c). However, expression was further increased when cells were infected with an HIV that lacked Vif expression (Fig. 1b). Data compiled from nine independent donors revealed a consistent and statistically significant increase in ligand expression that was on average 1.5 fold higher than wild type HIV infection (Fig. 1c). As previously reported, infection with an HIV lacking Nef also yielded higher ligand expression[23] (Fig. 1b and 1c). Infection of T cells with a virus lacking expression of both Vif and Nef resulted in ligand expression similar to that achieved with each single mutant suggesting that Vif and Nef were acting on the same pathway.

In contrast, mutation of Vpr reduced NKG2D ligand expression to that observed in uninfected cells (approximately three-fold lower than wild type virus, Fig. 1b and 1c), confirming that Vpr expression was required for HIV-mediated NKG2D ligand upregulation[20]. Examination of ligand expression by cells infected with *vif*$^{-}$*vpr*$^{-}$ and *nef*$^{-}$*vpr*$^{-}$ double mutant HIVs revealed that all of the additional ligand upregulation observed in the absence of Vif and Nef depended on Vpr expression (Fig. 1d and 1e).

To confirm that the ligand phenotype we observed was due to alteration in Vif expression by *vif*$^{-}$ HIV, we demonstrated that this phenotype could be rescued by a lentiviral vector expressing wild type *vif* in the HIV-infected target cells (Fig. 1f, left panel). The expression level of Vif we achieved with lentiviral transduction was less than wild type (Fig. 1g, left panel) and this difference may explain the partial rescue. In contrast, expression of Vif in the virus producing cells at amounts similar to that achieved with wild type HIV (Fig. 1g, right panel) did not significantly alter ligand expression of the infected cells (Fig. 1f, right panel). These data confirm that Vif expression in HIV infected target cells reduces Vpr-dependent NKG2D ligand upregulation.

A3G expression correlates with NKG2D ligand upregulation

Because Vif targets A3G for degradation, we asked whether the effects of Vif on NKG2D ligand expression were related to A3G. Amongst uninfected donors, the amount of baseline A3G protein were highly variable (Fig. 2a). In addition, we found that we could increase A3G expression by incubating the $CD56^{-}CD8^{-}$ target cells with conditioned supernatant from CD8-depleted PBMC cultures (Fig. 2a) according to the time line shown in Fig. 2b. We also noted that the surface expression of NKG2D ligands increased with this treatment (Fig. 2c, left panels). Variation in the amounts of A3G protein across donors correlated strongly with NKG2D ligand expression (Fig. 2d).

In some donors, we also observed an increase in the amount of A3G in primary T cells treated with viruses that lacked Vif expression or that contained a mutant Vif (Vif $Y_{44}A$) defective at binding and degrading A3G[24] (Fig. 2e - 2g). The increase in A3G protein with Vif $Y_{44}A$ was less than *vif*$^{-}$ viruses in some donors, potentially indicating this mutation was incompletely defective. Compared with *vif*$^{-}$ viruses there was no further effect of mutating *vpr* on A3G levels (Fig. 2g).

Furthermore, intracellular staining and flow cytometric analysis of a separate set of five donors revealed that A3G expression was higher in *vif*$^{-}$ HIV infected (Gag^{+}) cells compared to uninfected cells in the culture or mock infected cells (Fig. 2h, $p = 0.04$). These data support the conclusion that in the absence of Vif, HIV infection can induce A3G expression in the infected cell for the majority of donors.

Overall, we noted a strong positive correlation across multiple donors between A3G expression, as determined by immunoblotting, and the induction of NKG2D ligand expression for both infected and uninfected cells with a significant additional effect of infection (Fig. 2i, slope of regression lines significantly different, $p < 0.0001$). These data support the possibility that A3G expression determines the extent to which NKG2D ligands are upregulated.

We then examined NKG2D expression on cells infected with HIV expressing the $Y_{44}A$ mutant *vif*, which is unable to bind and degrade A3G. We found that cells infected with this mutant virus had similar NKG2D ligand protein as Vif-deficient virus in eight independent donors, indicating that Vif's ability to limit NKG2D ligand expression is secondary to its ability to bind A3G (Fig. 2j).

A3G activates the DNA damage response pathway

Recent reports have indicated that activation of the DNA damage response pathway can lead to increases in NK cell activating ligand expression[25]. DNA damage results in phosphorylation of the cyclin-dependent kinases ATR and ATM and phosphorylation of the checkpoint kinases Chk1 or Chk2 which inhibit cell cycle progression and promote DNA repair. Distinct types of damage activate these pathways. For example, ATR is activated in response to exposed stretches of single stranded DNA whereas ATM is activated in response to double stranded DNA breaks (reviewed in [26]).

To examine whether the DNA damage response pathway could be linked to A3G expression and/or upregulation of NKG2D ligands in HIV-infected cells, we measured the effect of HIV infection on Chk1 and Chk2 phosphorylation. We observed that HIV infection increased Chk2 phosphorylation several fold (Fig. 3a and 3b). Moreover, we noted further increases in phosphorylated Chk2 in cells infected with *vif*$^-$ HIVs (Fig. 3a and 3b). HIV infection also influenced Chk1 phosphorylation in some donors, although to a lesser degree than Chk2 (Fig. 3a and 3c). Notably, Chk2 phosphorylation was affected by HIV in a manner that mirrored the induction of NKG2D ligands in that it was Vpr-dependent and attenuated by Vif expression (compare Fig. 3b to Fig. 2j).

We also observed that the magnitude of Chk2 phosphorylation correlated across multiple donors with A3G expression in cells infected with *vif*$^-$ HIVs and mock infected control cells, but the slope of the regression line was significantly higher in HIV-infected cells (Fig. 3d, $p < 0.02$). In contrast, when A3G protein expression across multiple donors were compared to Chk1 phosphorylation there was no significant correlation and NL-PI*vif*$^-$ infected cells were indistinguishable from mock infected (Fig. 3e). While this suggests that Chk2 is more important than Chk1 for this response, higher background expression of Chk1 than Chk2 may limit our ability to detect changes in the infected subpopulation.

Based on the fact that A3G protein expression correlated best with Chk2 phosphorylation, we predicted that A3G was activating an ATM pathway. Consistent with this prediction, we observed an increase in ATM phosphorylation in HIV-infected cells and we found that ATM phosphorylation was enhanced in NL-PI*vif*$^-$ infected cells (Fig. 3f). In addition, we found that the ATM inhibitor KU55933 [27] significantly reduced NKG2D ligand upregulation by wild type and *vif*$^-$ HIVs when compared to solvent controls (Fig. 3g, $p = 0.03$ for NL-PI and $p = 0.02$ for *vif*$^-$). Furthermore, cells treated with the ATM inhibitor (KU55933) no longer displayed a significant increase in NKG2D ligands in NL-PI*vif*$^-$ infected cells compared to wild type virus infected cells, further indicating that A3G-mediated NKG2D ligand upregulation is ATM-dependent (Fig. 3g). However, total NKG2D ligand expression remained 3-fold higher in HIV-infected cells treated with KU55933 than mock-infected cells (Fig. 3g). The partial inhibition by KU55933 is consistent with the fact that Vpr can also upregulate NKG2D ligands via the ATR pathway[20].

To determine whether the observed increase in Chk2 phosphorylation in *vif*$^-$ HIV infected cells was also ATM-dependent, we measured Chk2 phosphorylation in KU55933 treated primary T cells infected with an HIV lacking Vif expression. As predicted, we found that KU55933 reduced the phosphorylation of Chk2 for *vif*$^-$ HIV infected primary T cells (Fig. 3h). These data support a model in which A3G upregulates NKG2D ligands through an ATM pathway and in which Vif counteracts this upregulation by reducing A3G expression.

A3G sensitizes HIV infected T cells to NK cell lysis

To assess the relevance of NK cell ligand expression on NK cell recognition of HIV infected cells and to determine whether Vif might protect infected cells from NK cell lysis by degrading A3G, we used a previously described flow cytometric killing assay[12]. In this assay system, target cells pre-labeled with carboxyfluorescein succinimidyl ester (CFSE) were incubated with media or unlabeled, highly purified, autologous NK cells. Immediately

afterward, the cell mixture was stained with antibodies directed against the NK cell markers CD16 and CD56 as well as the vital dye 7AAD to discriminate live and dead cells. The number of $7AAD^{-}CD16^{-}CD56^{-}CFSE^{+}$ cells was then scored as a function of a defined number of inert counting beads added just prior to flow cytometric analysis. When this assay system was tested using the highly sensitive K562 cells, which lack MHC-I and express high amounts of NK cell activating ligands, the addition of primary NK cells resulted in a dramatic reduction of living $CFSE^{+}$ target cells (Supplementary Fig. 1).

To assess NK cell lysis of HIV-infected primary T lymphocytes, we infected cells with HIV expressing a GFP reporter inserted within the *env* open reading frame (ORF) to distinguish infected from uninfected cells (Fig. 4a). On day two of infection, autologous NK cells were co-incubated with the infected cells for four hours and then analyzed to detect NK cell lysis as described for Supplementary Fig. 1. We found that a high fraction of HIV-infected primary T lymphocytes survived treatment with autologous NK cells, whereas K562 cells were completely killed (Fig. 4b, left panels and quantified in Fig. 4c). At the highest effector to target cell ratio tested, 47% of the HIV-infected primary T lymphocytes survived, compared with <1% survival of K562 cells (Fig. 4c).

To determine whether inefficient killing resulted from deficient NK cell activation, we constructed an HIV genome that overexpressed the NKG2D activating ligand, ULBP1 (NL-GI*ulbp1*$^{+}$) plus or minus a full-length *nef* open reading frame (Fig. 4a). Primary T cells infected with NL-GI*ulbp1*$^{+}$ expressed roughly 40-fold more ULBP1 on their surface compared to control infected cells (Fig. 4d). We found that ULBP1 overexpression enhanced NK cell clearance of HIV-infected cells approximately ten-fold, suggesting that NKG2D activating ligand expression was limiting for NK cell lysis of HIV-infected primary T cells (Fig. 4b, right panels and quantified in Fig. 4c).

We then asked whether overexpression of activating ligands would affect NK cell recognition of infected cells that had normal MHC-I expression. To test this, primary T cells were infected with *nef*$^{-}$ HIVs plus or minus ULBP1 overexpression. In the absence of ligand overexpression these cells were substantially more sensitive to NK cell lysis than mock infected cells, indicating that HIV infection activated NK cell lysis even without MHC-I downmodulation (Fig. 4e, left panels and quantified in Fig. 4f). These data are consistent with our observations that HIV infection upregulates NKG2D activating ligands. However, overexpression of NK cell activating ligands in infected cells further increased killing and resulted in loss of most of the remaining cells (Fig. 4e, right panels and Fig. 4f). These data indicate that at high amounts of NKG2D ligands, MHC-I downmodulation is not essential for efficient NK cell lysis.

To determine whether the inhibitory effect of Vif on NKG2D ligand upregulation was physiologically relevant, we asked whether Vif expression affected NK cell lysis of infected cells. An analysis of infected cells from five independent donors revealed that cells lacking Vif were significantly more sensitive to NK cell recognition than wild type HIV controls in a four hour cytotoxicity assay (Fig. 5a, mean survival 60% and 66% for wild type compared with 38% and 45% for infected cells lacking Vif were significantly more sensitive to NK cell recognition than cells infected with wild type HIV.

We then asked whether A3G expression influenced NK cell recognition by knocking down A3G with siRNA. To accomplish this, we constructed a lentiviral vector expressing an shRNA directed against A3G and GFP, which allowed us to gate on the knock-down cells and assess survival in the presence of NK cells using the flow cytometic killing assay. As a control, we determined that the shRNA containing vector could significantly reduce A3G expression in transfected 293 cells (Fig. 5b).

When primary T cells were co-transduced with shA3G or shNC expressing lentiviruses and *vif* $^{-}$ HIV, we found that A3G knock down significantly improved survival of infected cells co-incubated with autologous NK cells (p=0.02, n= 3, Fig. 5c and 5d). These data indicate that A3G sensitizes infected cells to NK lysis and that Vif-dependent A3G degradation likely explains Vif's protective effect (Fig. 5a).

Vif and Vpr reduce uridine incorporation

Because A3G deaminates cytosine to uracil, it is possible that the presence of uracil in DNA is sufficient to cause upregulation of NK activating ligands. Alternatively, gaps and breaks created by the cellular repair of uridine containing DNA could be responsible. To distinguish between these two possibilities, we directly measured the effect of Vpr and Vif on uridine incorporation. The assay we developed to measure uridine incorporation utilizes the activity of recombinant uracil DNA glycosylase (UDG), which specifically removes uracils, creating an abasic site that no longer serves as a template for PCR. In this assay, uridine incorporation is detected by a relative reduction in amplification of the template following UDG treatment. As a control, we generated uridine-containing and non-uridine containing PCR products and demonstrated that amplification of templates containing uridine was specifically inhibited by UDG treatment (Fig. 6a).

When we examined DNA prepared from infected primary T cells, UDG treatment did not affect amplification of wild type (NL-PI) HIV proviral DNA, indicating that there was no detectable uridine in this sample. However, a significant effect of UDG on the amplification of HIV proviral DNA from *vif* $^{-}$ *vpr* $^{-}$ infected cells (Fig. 6b, compared to theoretical mean of 1.0, $p = 0.03$), indicating the presence of uridine in the DNA from this sample. There was no significant effect of UDG on amplification of proviral DNA from cells infected with either of the single mutants, suggesting that Vif and Vpr can independently limit uridine incorporation.

We noted a similar pattern of sensitivity to UDG when we amplified sequences from a cellular gene (β-actin) (Fig. 6b, compared to theoretical mean of 1.0, $p = 0.02$ and $p = 0.0006$ for *vif* $^{-}$ and *vif* $^{-}$*vpr* $^{-}$, respectively) and UDG sensitivity positively correlated with infection rate for DNA isolated from *vif* $^{-}$ *vpr* $^{-}$ HIV infected cells (Fig. 6c). Thus, these data indicate uridine incorporation can also occur in cellular genomic DNA isolated from infected cells.

We also recovered significantly less HIV DNA from cells infected with *vif* $^{-}$*vpr* $^{-}$ HIV relative to wild type HIV after normalizing for infection rate and cellular DNA content (Fig. 6d). By comparison, the relative amounts of cellular DNA recovered from each sample, as measured by amplification of β-actin was somewhat increased with infection by this mutant

(Fig. 6e). The relatively low recovery of *vif*⁻*vpr*⁻ HIV DNA was not explained by differences in the ability of the polymerase to amplify uridine-containing DNA; control uridine-containing templates were amplified as efficiently as non-uridine containing templates (Fig. 6f). Thus, *vif*⁻*vpr*⁻ provirus appears to be less stable following infection of primary T cells. The synergistic effect of mutating both Vif and Vpr is consistent with our hypothesis that both proteins act on the same pathway to stabilize provirus.

Vpr-UNG2 interaction and NKG2D ligand upregulation

Based on the fact that uridine was only detectable in cells infected with *vif*⁻*vpr*⁻ HIV and the fact that cells infected with *vif*⁻*vpr*⁻ HIV have low ligand expression, we concluded that uridine itself was not sufficient to induce ligand expression. Thus, we hypothesized that it was the repair of uridine containing DNA that was responsible for Vpr and A3G-dependent NK cell activating ligand upregulation. In this model the effects of Vpr on NKG2D ligand expression would be mediated by interaction with uracil glycosylase, UNG2. To test this, we constructed HIVs that contained a Vpr with a mutation in the UNG2 binding domain (Vpr $W_{54}R$)[28]. The Vpr phenotype is masked in the presence of Vif or Nef (Fig. 1c and 1e). Therefore, to focus on a potential Ung2 binding phenotype, we tested the Vpr mutant in a *nef*– background. As predicted, we found that this mutant was less active at inducing NK activating ligand expression compared with wild type Vpr (Fig. 7a, $p = 0.0004$), indicating that at least a component of Vpr's effect on ligand expression required UNG2 binding. Mutating the UNG2 binding site of Vpr did not completely eliminate NKG2D ligand upregulation, thus we cannot rule out the possibility that Vpr also upregulates ligands through interactions with other cellular factors, such as SMUG1.

To confirm a role for UNG2, we knocked down UNG2 expression and assayed for NKG2D ligands in HIV-infected primary T lymphocytes. UNG2 expression was reduced 85% in CEM-SS T cells with UNG2-specific shRNA compared to control treated cells (Fig. 7b). Consistent with our model, knockdown of UNG2 in primary T cells also reduced the upregulation of NKG2D ligands by wild type HIV compared to control treated (Fig. 7c, $p = 0.03$). Once again, complete inhibition of NKG2D ligand expression was not observed by knocking down UNG2 expression, potentially implicating other cellular factors. In sum however, these data support a model in which Vpr induces NKG2D ligand upregulation in HIV infected T cells by stimulating UNG2-dependent repair of uridine-containing DNA (Supplementary Fig. 2).

Discussion

Members of the APOBEC and AID family of cytidine deaminases are key host factors that aid in the defense against pathogens. There is growing evidence for overlapping roles of these deaminases in alerting killer T cells to infection and DNA damage. For example, A3G has been shown to stimulate CTL recognition through the generation of defective translation products[29]. In addition, the "DNA damage" resulting from AID-mediated somatic hypermutation leads to upregulation of NK cell activating ligands that transiently mark these cells as potentially dangerous[30]. We now show that, like AID, A3G expression sensitizes cells to NK cell recognition through the upregulation of NKG2D ligand expression in HIV

infected cells. A3G knockdown increased the survival of cells infected with a Vif-deficient HIV and incubated with autologous NK cells. In addition, wild type Vif inhibited NKG2D ligand expression whereas Vif mutants defective at binding and degrading A3G did not. It is intriguing to speculate that these effects on NKG2D ligands may also contribute to A3G-dependent enhancement of CTL recognition[29], as NKG2D can serve as a co-stimulatory molecule in CTLs[31].

The effect of AID on the DNA damage response is related to its cytidine deaminase activity that results in uridine incorporation into cellular genomic DNA. Removal of the uracil by UNG2 and AP endonucleases generates gaps and breaks that lead to activation of the DNA damage response[32]. In contrast to AID, A3G is a cytoplasmic protein that targets ssDNA and it is less clear how its expression could lead to the incorporation of uridine into double stranded cellular DNA and activate the nuclear DNA damage response. Indeed, a recent publication did not detect an effect of A3G on mutation rate of transfected HEK 293 cells[33]. Thus, the ability of A3G to access cellular DNA appears to be specific to HIV-infected primary T cells lacking Vpr and Vif. The finding that Vif and Vpr specifically inhibit uracilation of cellular DNA suggests this is an important cellular response that HIV has evolved to evade.

Although A3G targets single stranded DNA, and most cellular DNA is double stranded, short stretches of dsDNA have the propensity to temporarily dissociate or “breathe” [34], and these may be targeted by A3G in infected cells. In addition, it remains possible that other cytidine deaminases, some of which are nuclear and able to target double stranded DNA[33], contribute to uracilation of cellular DNA in the setting of HIV infection. Importantly, in the absence of Vpr and Vif we not only observed uracilation but also instability of HIV DNA. Thus, the in-coming HIV-1 genome is likely the primary target of this response, which results in uracilation followed by degradation of the HIV-1 DNA in the absence of Vpr and Vif.

We also show here that maximal upregulation of NKG2D ligands and the DNA damage response requires Vpr in addition to A3G. One model that explains the combined effects of Vpr and A3G is that Vpr expression is required to promote the repair of A3G-generated mutations through its interaction with UNG2 [28]. This model is consistent with prior studies demonstrating that Vpr reduces the requirement for high Vif expression in the presence of A3G[21]. Moreover, NKG2D ligand upregulation was reduced when the UNG2 binding site of Vpr was mutated or UNG2 expression was knocked down. Complete reversal of NKG2D ligand expression was not observed when UNG2 expression was reduced, either because of incomplete knockdown or because other factors can substitute for UNG2 activity.

Repair of integrated uridines reduces the error rate and improves the infectivity of progeny virus. However, the repair process, which generates nicks, gaps and breaks, has the side effect of activating an ATM response that results in NKG2D ligand upregulation. The link between NKG2D ligand upregulation and deamination reveals broader implications of the intrinsic antiviral response mediated by APOBEC proteins than had previously been appreciated. Indeed, it appears that the A3G response to infection includes the initiation of a cellular suicide mission meant to contain viral production and spread.

The importance of uridine incorporation as an innate immune response is made clear by the fact that a wide range of viruses encode mechanisms to avoid it[35]. In addition, HIV-1 recruits UNG2 to virions, which has been reported to enhance viral infectivity by limiting dUTP misincorporation during reverse transcription[36] and to excise uridines resulting from A3G-editing[37]. Thus, there may be multiple routes through which HIV limits uridine incorporation.

When prior studies have measured the effect of A3G on viral particle inactivation, it was clear that A3G made in the producer cells and packaged into newly formed virions was required for viral inactivation and that A3G in the target cells was dispensable[7]. However, we provide evidence here that A3G expressed in the target cell also plays a role in the innate immune response. While A3G present in the target cell may be insufficient to inhibit the invading virus from productively infecting the cell, our data indicate that A3G expression in target cells is required for sensitization of HIV-infected cells to NK cell lysis.

We also report here that treatment of primary T cells with Vif-deficient HIV-containing cell supernatants resulted in an increase in A3G expression in HIV infected cells in some donors. This response has not previously been reported and the mechanism is unknown. Influenza virus ssRNA also increases A3G expression[38]. Although the mechanism for this increase is unclear, HIV-1 single stranded RNA binds Toll-like receptors 7 and 8[39]. Pathogen recognition receptor ligation induces type I interferon production, which stimulates A3G expression[2]. Our results highlight the possibility that detection of HIV by the innate immune system could lead to the production of A3G in infected cells.

In sum, the data presented here demonstrate that A3G expression enhances recognition of HIV-infected cells by NK cells through upregulation of NKG2D activating ligands. Thus, therapeutic strategies aimed at augmenting the anti-viral activity of A3G may have the added benefit of promoting immune clearance of virally infected cells by NK cells.

Methods

Cell culture and viral infections

We obtained pre-existing leukopaks lacking subject identifiers from The New York Blood Center. The use of these specimens was reviewed by the University of Michigan IRB and found not to be human subjects research. We isolated PBMCs by Ficoll-Paque density separation. We prepared $CD56^+$ NK cells from adherence-depleted PBMCs using commercially available kits (EasySep, StemCell Technologies). After isolation we maintained $CD56^+$ cells in RPMI 1640 with 10% human AB serum (Fisher scientific), penicillin, streptomycin, L-glutamine and 500 IU/ml rhIL-2[42]. PBMCs were prepared for HIV infection as previously described[14] except that they were also CD56-depleted (EasySep, StemCell Technologies). Virus production and infection of PBMCs have been previously described[12, 43]

Viral constructs

HIV NL-PI and *nef*$^-$, *vpr*$^-$, *vpu*$^-$, *vpr*$^-$*nef*$^-$ accessory protein mutants have been reported previously[12, 40]. *Vif* expression was disrupted by filling in the NdeI site at position 83 of *vif*.

Nef expression was disrupted by filling in the XhoI site at position 101 of *nef*. We used a standard PCR-based mutagenesis strategy to generate NL-PI*vif*Y_{44}A and NL-PI*vpr*W_{54}R (see primers in Table S1).

FG12 shA3G and shUNG2, short hairpin RNA expression constructs targeting APOBEC3G and UNG2, were cloned using the primers in Table S1 into the lentiviral vector FG12[44] as described previously[43]. The negative control vector (FG12 shNC) was previously described[43].

To construct the Vif FG9 lentiviral expression vector, NL4-3 Vif was amplified by PCR (see primers in Table S1) and cloned into the BamHI and NotI sites of FG9[45].

To construct pNL-GI*ulbp1*$^{+}$, *ulbp* was amplified from cDNA (MegaMan Human Trascriptome Library, Stratagene; Table S1) and a PCR-based strategy was used to create the IRES*ulbp1* cassette from the amplicon (**see primers in** Table S1). The cassette was cloned into the NheI and BglII sites in the *env* open reading frame of pNL-G (pNL4-3-deltaE-EGFP)[41].

Flow cytometry

Cell surface proteins (aside from NKG2D ligands), were stained in flow cytometry buffer plus human serum (PBS with 2% FBS, 1% human type AB serum, 1% HEPES and 1% NaN_3) using the antibodies listed in Table S2 and fluorescently conjugated isotype-specific secondary antibodies (Invitrogen or Caltag), then fixed in 2% paraformaldehyde. For NKG2D ligand analysis, cells were stained with rhNKG2Dfc (R&D Systems) and anti-CD3 antibody (Table S2) in flow cytometry buffer without human serum. Intracellular Gag stains were performed as previously described[46]. For A3G staining, cells were fixed and permeabilized in 90% methanol, blocked in PBS-1% BSA-10% goat serum prior to staining with APOBEC3G antibody (Abcam) or normal rabbit serum control (Santa-Cruz) in PBS-1% BSA. Cells were subsequently stained for Gag and FITC or GAR-488 conjugated anti-rabbit secondary antibodies (Biosource and Invitrogen) diluted in PBS-1% BSA for 30 min RT.

NK cell cytotoxicity

Target cells (K562 cells and HIV-1 infected and mock treated primary T lymphocytes) were labeled with 500 μM CFSE (Invitrogen) one day prior to the NK cell assay and incubated overnight at 37°C. Alternatively, target cells were infected with FG12 shRNA or NL-G viruses expressing GFP. Labeled target cells were co-incubated with purified, autologous NK cells at increasing effector:target ratios for 4 hours at 37°C and then stained for surface MHC-I, PLAP, CD56, CD16 and 7-amino actinomycin D (7-AAD, Calbiochem) and analyzed by flow cytometry. Live target cells were identified by light scatter parameters, 7-AAD exclusion, and $CD56^{-}/CD16^{-}/CFSE^{+}$(or GFP) staining. A constant number of fluorescent counting beads (Countbright beads, Invitrogen) was added to each tube and counted during cytometric acquisition. The normalized number of live cells was calculated as the number of cells times the fraction of beads counted. Percent target cell survival was determined as the percent normalized target cells remaining after NK cell incubation.

Immunoblot Analysis

48 hours post HIV infection, PBMC lysates were isolated as previously described[47]. Normalized whole cell lysates were analyzed by immunoblot using the antibodies in Table S2. APOBEC3G[48] and Vif[49] antibodies were previously described. Membranes were incubated with HRP-conjugated secondary antibodies (Invitrogen) and developed. Background-subtracted median band intensities were determined using Adobe Photoshop and normalized to tubulin for quantification.

Quantitative PCR analysis

Infected cells were harvested 48 hours post-infection. For DNA extraction, cells were resuspended in PBS and lysed with MagNa Pure Lysis/Binding buffer (Roche). Lysed cells were loaded on the MagNa Pure Compact and total DNA was extracted. Samples were treated with 10U UDG (NEB) and incubated at 37°C for 1h followed by 10 minutes at 95°C to inactivate the UDG. For samples with heat-inactivated UDG, DNA was added after UDG heat-inactivation.

For qPCR analysis, the TaqMan ProbeMaster kit (Roche) and the primers in Table S3 were used. HIV-1 DNA was first subjected to 12 cycles of linear amplification using the 2^{nd}-LTR-F-univ primer[46] to amplify the negative strand. Probe-2 was previously described[50].

Control TTP and UTP-containing templates were generated by PCR amplifying NL-PI using the 2^{nd}-LTR-F and Gag-R-3 primers. For UTP control templates, dUTP instead of dTTP was used. Gel purified TTP and UTP-containing control templates were analyzed post UDG treatment by gel electrophoresis of re-amplified samples

Statistical analysis

Statistical significance in the flow cytometry and western blot data were assessed by paired *t* test. Regression analysis was performed using GraphPad Prism software.

For qPCR data, amplification efficiency (E) was calculated as E = 10^(−1/slope of target standard curve) – 1. Average Cq for three replicates of each sample was converted to Cq at 100% efficiency (Cq_{100}) = Cq*Log_2(1+E) to permit comparison between different genes. ΔCt values for each sample were calculated as Cq_{100}(untreated) – Cq_{100}(UDG treated) and converted to quantity ratios (2^ΔCt). One sample t-tests were used to compare ΔCts and quantity ratios to the expected values if UDG treatment has no effect: 0 and 1, respectively. Total HIV-1 DNA was assessed by computing ΔCt values for non-UDG treated samples relative to beta-actin and Ct values comparing each mutant virus to NL-PI. Ct values were converted to quantity ratios and normalized to infection rate. One sample t-tests were used to compare the normalized quantity ratios to the expected value of 1 if HIV-1 DNA amplification does not vary with Vif or Vpr mutation.

Supplementary Material

Refer to Web version on PubMed Central for supplementary material.

Acknowledgements

This work was funded by U.S. National Institutes of Health Grant RO1 AI051192. LAM was supported by U.S. National Science Foundation Graduate Student Research Fellowship under Grant DGE 0718128. MM was supported by U.S. National Institutes of Health grants T32GM007863 and T32AI007413. AON was supported by U.S. National Institutes of Health grant UL1RR024986 from the National Center for Research Resources. Services were provided by the University of Michigan Flow Cytometry core, Sequencing Core (supported by National Institutes of Health grant P30CAO46592), Hybridoma Core (supported by National Institutes of Health grant P30AR048310) and Center for Statistical Consultation. The content is solely the responsibility of the authors and does not necessarily represent the official views of NCRR or the National Institutes of Health. The following reagents were obtained through the AIDS Research and Reference Reagent Program, Division of AIDS, National Institute of Allergy and Infectious Diseases, US National Institutes of Health: Human rIL-2 from Dr. Maurice Gately, Hoffmann (La Roche Inc), pNL4–3–deltaE–EGFP (Cat# 11100) from Drs. Haili Zhang, Yan Zhou, and Robert Siliciano (Johns Hopkins University), APOBEC3G antiserum (ApoC17) from Dr. Klaus Strebel (NIAID, NIH), HIV-1 Vif monoclonal antibody (#319) from Dr. Michael H. Malim (King's College London), and HIV-1_{SF2} p24 antiserum.

References

1. Deeks SG, Walker BD. Human immunodeficiency virus controllers: mechanisms of durable virus control in the absence of antiretroviral therapy. Immunity. 2007; 27:406–416. [PubMed: 17892849]
2. Peng G, Lei KJ, Jin W, Greenwell-Wild T, Wahl SM. Induction of APOBEC3 family proteins, a defensive maneuver underlying interferon-induced anti-HIV-1 activity. The Journal of experimental medicine. 2006; 203:41–46. [PubMed: 16418394]
3. Chiu Y-L, Greene WC. The APOBEC3 cytidine deaminases: an innate defensive network opposing exogenous retroviruses and endogenous retroelements. Annual review of immunology. 2008; 26:317–353.
4. Zhang H, et al. The cytidine deaminase CEM15 induces hypermutation in newly synthesized HIV-1 DNA. Nature. 2003; 424:94–98. [PubMed: 12808465]
5. Bishop KN, Verma M, Kim E-Y, Wolinsky SM, Malim MH. APOBEC3G inhibits elongation of HIV-1 reverse transcripts. PLoS Pathogens. 2008; 4:e1000231. [PubMed: 19057663]
6. An P, et al. APOBEC3G genetic variants and their influence on the progression to AIDS. J Virol. 2004; 78:11070–11076. [PubMed: 15452227]
7. Yu X, et al. Induction of APOBEC3G ubiquitination and degradation by an HIV-1 Vif-Cul5-SCF complex. Science (New York, NY). 2003; 302:1056–1060.
8. Kijak GH, et al. Variable contexts and levels of hypermutation in HIV-1 proviral genomes recovered from primary peripheral blood mononuclear cells. Virology. 2008; 376:101–111. [PubMed: 18436274]
9. Jern P, Russell R, Pathak V, Coffin J. Likely role of APOBEC3G-mediated G-to-A mutations in HIV-1 evolution and drug resistance. PLoS Pathogens. 2009; 5:e1000367. [PubMed: 19343218]
10. Goulder PJR, Watkins DI. Impact of MHC class I diversity on immune control of immunodeficiency virus replication. Nature Reviews Immunology. 2008; 8:619–630.
11. Schwartz O, Maréchal V, Le Gall S, Lemonnier F, Heard JM. Endocytosis of major histocompatibility complex class I molecules is induced by the HIV-1 Nef protein. Nature Medicine. 1996; 2:338–342.
12. Collins KL, Chen BK, Kalams SA, Walker BD, Baltimore D. HIV-1 Nef protein protects infected primary cells against killing by cytotoxic T lymphocytes. Nature. 1998; 391:397–401. [PubMed: 9450757]
13. Martin MP, et al. Innate partnership of HLA-B and KIR3DL1 subtypes against HIV-1. Nat. Genet. 2007; 39:733–740. [PubMed: 17496894]
14. Le Gall S, et al. Nef interacts with the mu subunit of clathrin adaptor complexes and reveals a cryptic sorting signal in MHC I molecules. Immunity. 1998; 8:483–495. [PubMed: 9586638]
15. Jennes W, et al. Cutting edge: resistance to HIV-1 infection among African female sex workers is associated with inhibitory KIR in the absence of their HLA ligands. J Immunol. 2006; 177:6588–6592. [PubMed: 17082569]

16. Martin MP, et al. Epistatic interaction between KIR3DS1 and HLA-B delays the progression to AIDS. Nat. Genet. 2002; 31:429–434. [PubMed: 12134147]
17. Morvan M, et al. Phenotypic and functional analyses of KIR3DL1+ and KIR3DS1+ NK cell subsets demonstrate differential regulation by Bw4 molecules and induced KIR3DS1 expression on stimulated NK cells. J Immunol. 2009; 182:6727–6735. [PubMed: 19454667]
18. Champsaur M, Lanier L. Effect of NKG2D ligand expression on host immune responses. Immunological reviews. 2010
19. Fogli M, et al. Lysis of endogenously infected CD4+ T cell blasts by rIL-2 activated autologous natural killer cells from HIV-infected viremic individuals. PLoS Pathogens. 2008; 4:e1000101. [PubMed: 18617991]
20. Ward J, et al. HIV-1 Vpr triggers natural killer cell-mediated lysis of infected cells through activation of the ATR-mediated DNA damage response. PLoS Pathogens. 2009; 5:e1000613. [PubMed: 19798433]
21. Schröfelbauer B, Yu Q, Zeitlin SG, Landau NR. Human immunodeficiency virus type 1 Vpr induces the degradation of the UNG and SMUG uracil-DNA glycosylases. Journal of Virology. 2005; 79:10978–10987. [PubMed: 16103149]
22. Mansky LM, Preveral S, Selig L, Benarous R, Benichou S. The interaction of vpr with uracil DNA glycosylase modulates the human immunodeficiency virus type 1 In vivo mutation rate. Journal of Virology. 2000; 74:7039–7047. [PubMed: 10888643]
23. Cerboni C, et al. Human immunodeficiency virus 1 Nef protein downmodulates the ligands of the activating receptor NKG2D and inhibits natural killer cell-mediated cytotoxicity. J. Gen. Virol. 2007; 88:242–250. [PubMed: 17170457]
24. Russell RA, Pathak VK. Identification of two distinct human immunodeficiency virus type 1 Vif determinants critical for interactions with human APOBEC3G and APOBEC3F. J Virol. 2007; 81:8201–8210. [PubMed: 17522216]
25. Gasser S, Orsulic S, Brown E, Raulet D. The DNA damage pathway regulates innate immune system ligands of the NKG2D receptor. Nature. 2005; 436:1186–1190. [PubMed: 15995699]
26. Branzei D, Foiani M. Regulation of DNA repair throughout the cell cycle. Nat Rev Mol Cell Biol. 2008; 9:297–308. [PubMed: 18285803]
27. Hickson I, et al. Identification and characterization of a novel and specific inhibitor of the ataxia-telangiectasia mutated kinase ATM. Cancer Res. 2004; 64:9152–9159. [PubMed: 15604286]
28. Mansky LM, Preveral S, Selig L, Benarous R, Benichou S. The interaction of vpr with uracil DNA glycosylase modulates the human immunodeficiency virus type 1 In vivo mutation rate. J Virol. 2000; 74:7039–7047. [PubMed: 10888643]
29. Casartelli N, et al. The antiviral factor APOBEC3G improves CTL recognition of cultured HIV-infected T cells. Journal of Experimental Medicine. 2009
30. Gourzi P, Leonova T, Papavasiliou FN. A role for activation-induced cytidine deaminase in the host response against a transforming retrovirus. Immunity. 2006; 24:779–786. [PubMed: 16782033]
31. Maasho K, Opoku-Anane J, Marusina AI, Coligan JE, Borrego F. NKG2D is a costimulatory receptor for human naive CD8+ T cells. Journal of immunology (Baltimore, Md : 1950). 2005; 174:4480–4484.
32. Schrader CE, Linehan EK, Mochegova SN, Woodland RT, Stavnezer J. Inducible DNA breaks in Ig S regions are dependent on AID and UNG. The Journal of experimental medicine. 2005; 202:561–568. [PubMed: 16103411]
33. Stenglein MD, Burns MB, Li M, Lengyel J, Harris RS. APOBEC3 proteins mediate the clearance of foreign DNA from human cells. Nature Structural & Molecular Biology. 2010; 17:222–229.
34. Altan-Bonnet G, Libchaber A. Bubble dynamics in double-stranded DNA. Physical review letters. 2003; 90:138101. [PubMed: 12689326]
35. Sire J, Quérat G, Esnault C, Priet S. Uracil within DNA: an actor of antiviral immunity. Retrovirology. 2008; 5:45. [PubMed: 18533995]
36. Priet S, et al. HIV-1-associated uracil DNA glycosylase activity controls dUTP misincorporation in viral DNA and is essential to the HIV-1 life cycle. Mol Cell. 2005; 17:479–490. [PubMed: 15721252]

37. Yang B, Chen K, Zhang C, Huang S, Zhang H. Virion-associated uracil DNA glycosylase-2 and apurinic/apyrimidinic endonuclease are involved in the degradation of APOBEC3G-edited nascent HIV-1 DNA. J Biol Chem. 2007; 282:11667–11675. [PubMed: 17272283]

38. Pauli E-K, et al. High level expression of the anti-retroviral protein APOBEC3G is induced by influenza A virus but does not confer antiviral activity. Retrovirology. 2009; 6:38. [PubMed: 19371434]

39. Heil F, et al. Species-specific recognition of single-stranded RNA via toll-like receptor 7 and 8. Science. 2004; 303:1526–1529. [PubMed: 14976262]

40. Collins KL, Baltimore D. HIV's evasion of the cellular immune response. Immunol. Rev. 1999; 168:65–74. [PubMed: 10399065]

41. Zhang H, et al. Novel single-cell-level phenotypic assay for residual drug susceptibility and reduced replication capacity of drug-resistant human immunodeficiency virus type 1. J. Virol. 2004; 78:1718–1729. [PubMed: 14747537]

42. Lahm HW, Stein S. Characterization of recombinant human interleukin-2 with micromethods. J. Chromatogr. 1985; 326:357–361. [PubMed: 3875623]

43. Schaefer MR, Wonderlich ER, Roeth JF, Leonard JA, Collins KL. HIV-1 Nef targets MHC-I and CD4 for degradation via a final common beta-COP-dependent pathway in T cells. PLoS Pathogens. 2008; 4:e1000131. [PubMed: 18725938]

44. Qin X-F, An DS, Chen ISY, Baltimore D. Inhibiting HIV-1 infection in human T cells by lentiviral-mediated delivery of small interfering RNA against CCR5. Proc Natl Acad Sci USA. 2003; 100:183–188. [PubMed: 12518064]

45. Galbán S, et al. Cytoprotective effects of IAPs revealed by a small molecule antagonist. The Biochemical journal. 2009; 417:765–771. [PubMed: 18851715]

46. Carter CC, et al. HIV-1 infects multipotent progenitor cells causing cell death and establishing latent cellular reservoirs. Nature Medicine. 2010

47. Nakai-Murakami C, et al. HIV-1 Vpr induces ATM-dependent cellular signal with enhanced homologous recombination. Oncogene. 2007; 26:477–486. [PubMed: 16983346]

48. Kao S, et al. The human immunodeficiency virus type 1 Vif protein reduces intracellular expression and inhibits packaging of APOBEC3G (CEM15), a cellular inhibitor of virus infectivity. Journal of Virology. 2003; 77:11398–11407. [PubMed: 14557625]

49. Simon JH, Southerling TE, Peterson JC, Meyer BE, Malim MH. Complementation of vif-defective human immunodeficiency virus type 1 by primate, but not nonprimate, lentivirus vif genes. Journal of Virology. 1995; 69:4166–4172. [PubMed: 7769676]

50. Yamamoto N, et al. Analysis of human immunodeficiency virus type 1 integration by using a specific, sensitive and quantitative assay based on real-time polymerase chain reaction. Virus genes. 2006; 32:105–113. [PubMed: 16525741]

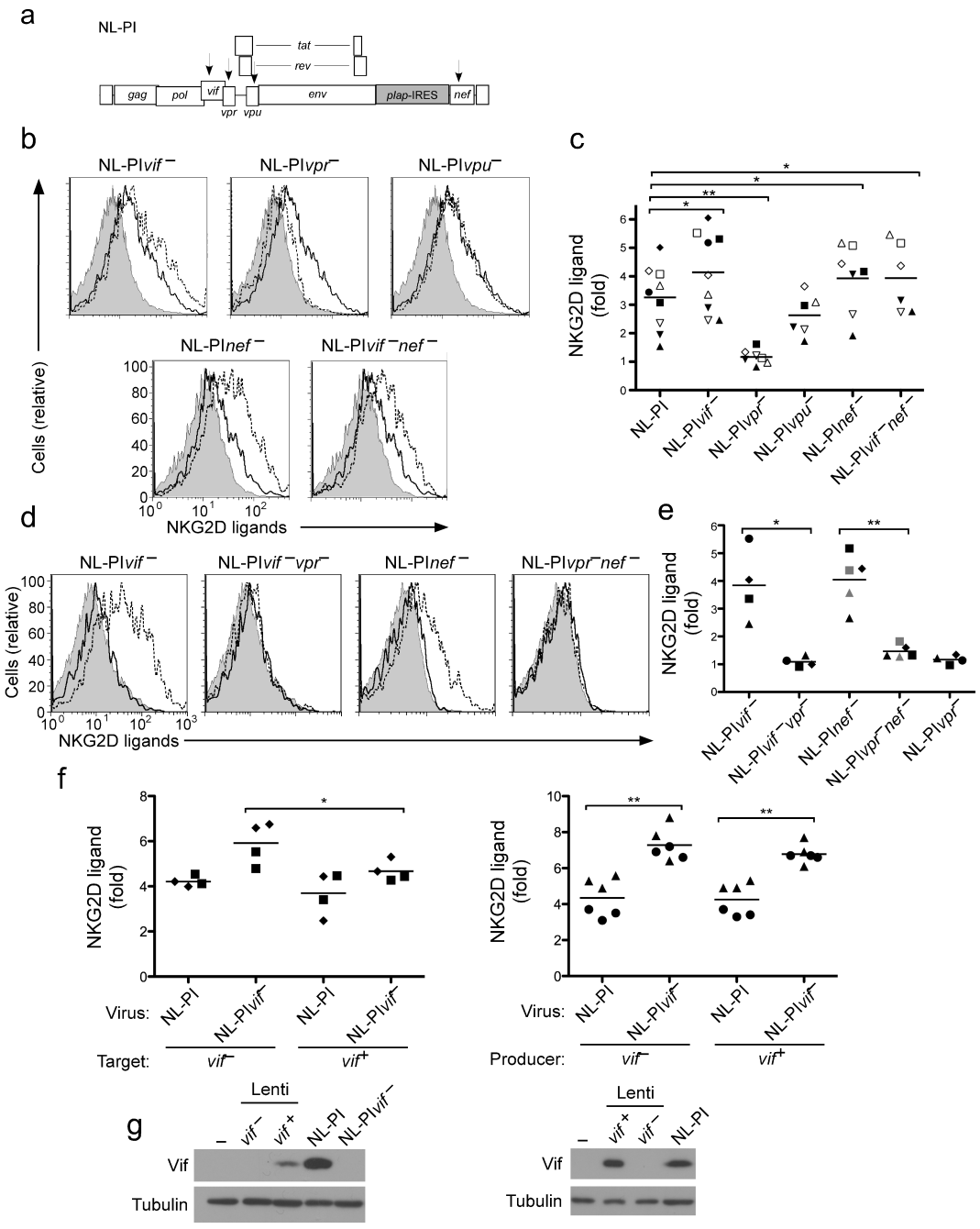

Figure 1. NKG2D ligand expression in HIV infected cells

(**a**) HIV genome of NL-PI, which has been previously described[12, 40]. Locations of mutations in individual ORFs are indicated. **(b-f)** Flow cytometric analysis of NKG2D ligand expression by $CD3^+$ T cells. Cells infected with NL–PI (solid black line), NL–PI accessory protein mutants (dashed black line) and mock-treated control (shaded gray histogram) are shown in part **(b)** whereas cells infected with NL–PI*vpr*$^-$ (solid black line), the indicated NL–PI accessory protein mutant (dashed black line) and mock-treated controls (shaded gray histogram) are presented in part **(d)**. **(c and e)** Summary plots of NKG2D

ligand expression on infected versus mock-infected T cells. The fold difference in NKG2D ligand expression relative to mock-treated controls is shown for independent donors, each represented by a different character. Black bars represent the mean fold change in ligand expression for each virus. Statistical analyses were calculated by paired *t* test. * $p<0.05$, ** $p<0.01$. **(f)** Summary plots of NKG2D ligand expression on NL-PI or NL-PI*vif*$^{-}$ infected primary T cells with or without Vif rescue. Left panel, primary T cells co-transduced with NL-PI or NL-PI*vif*$^{-}$ and *vif*-expressing or control lentiviruses. Right panel, viruses used to infect primary T cells were prepared from *vif*-expressing or control 293T cells. Two independent donors assayed in triplicate are shown. * $p<0.05$, ** $p<0.01$. **(g)** Immunoblot analysis of whole cell lysates from primary T cell targets (left panel) and 293T producer cells (right panel). Data are representative of two independent donors.

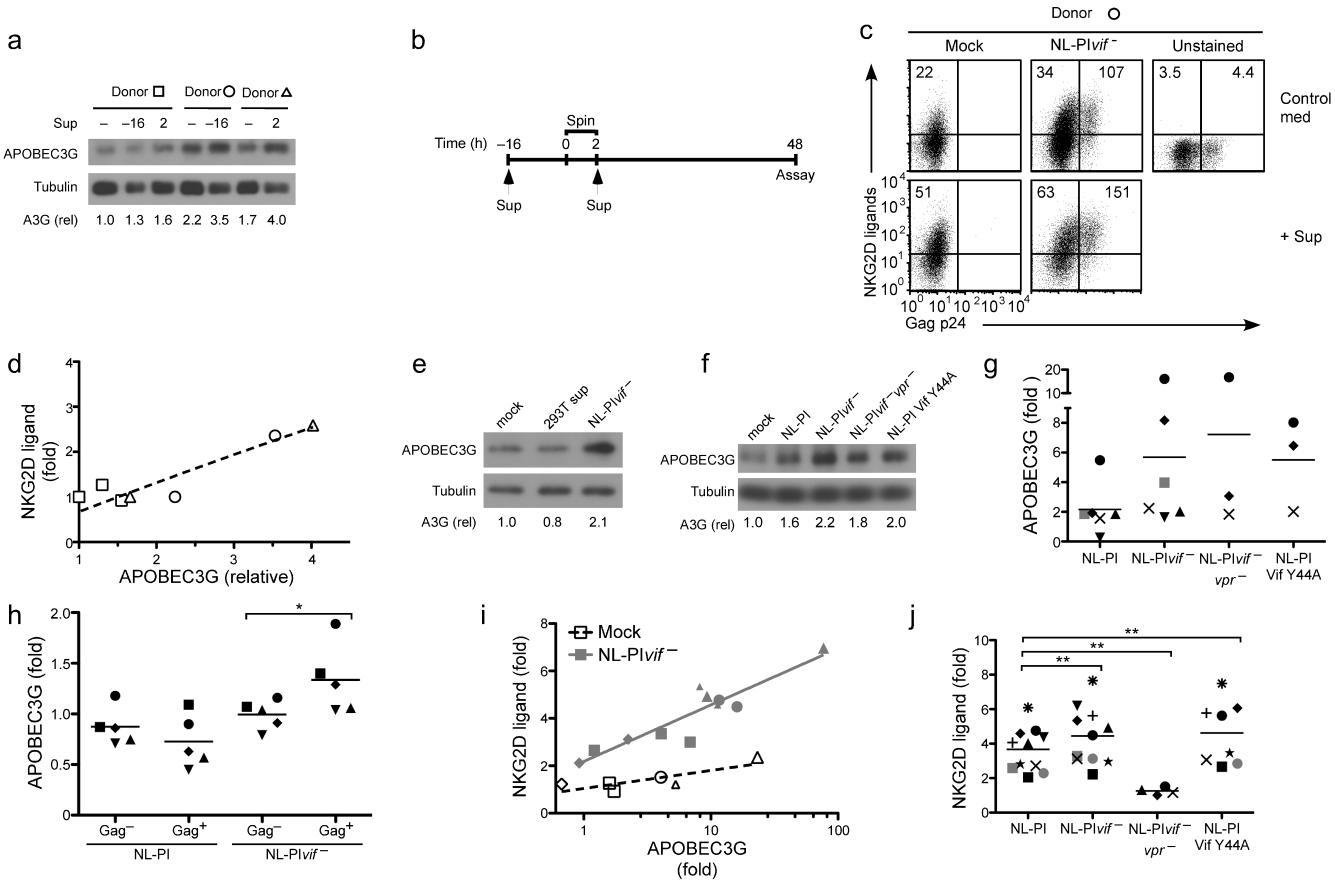

Figure 2. Upregulation of A3G correlates with NKG2D ligand upregulation

(a) Immunoblot analysis of T cells treated with media alone (−) or conditioned supernatant (Sup) (−16hr or 2hr) according to the experimental timeline in part **(b)**. **(c)** Flow cytometric analysis of $CD3^+$ T cells treated with conditioned supernatant (Sup) or control media (Control med) and infected with the indicated virus. The mean fluorescence intensity is indicated for the total Gag^- and Gag^+ populations. **(d)** Plot of relative A3G expression from part **(a)** versus NKG2D ligand normalized to control media treated cells. The linear best-fit line is indicated (R^2=0.83). **(e and f)** Immunoblot analysis of T cells infected with the indicated virus, control media (mock) or 293T cell supernatant. Data are representative of three independent donors. **(g and h)** Plot of relative A3G expression determined by **(g)** Immunoblot or **(h)** flow cytometric analysis of permeabilized cells infected with the indicated virus. Data obtained from each donor is indicated by unique symbols. *p<0.05 Donors in part **(g)** and **(h)** are independent. The mean fold change is indicated by the black bars. **(i)** Plot of A3G expression versus NKG2D ligand expression of mock-infected (white symbols) or NL-PIvif^- infected (gray symbols) cells with each independent donor indicated by a different symbol. R^2 for mock-infected =0.66, NL-PIvif^- R^2=0.84. **(j)** Summary of NKG2D ligand expression by cells infected with wild type or mutant NL-PI. Black bars indicate mean change in ligand expression. Each symbol represents a unique donor independent of those shown in Fig. 1. **p<0.02.

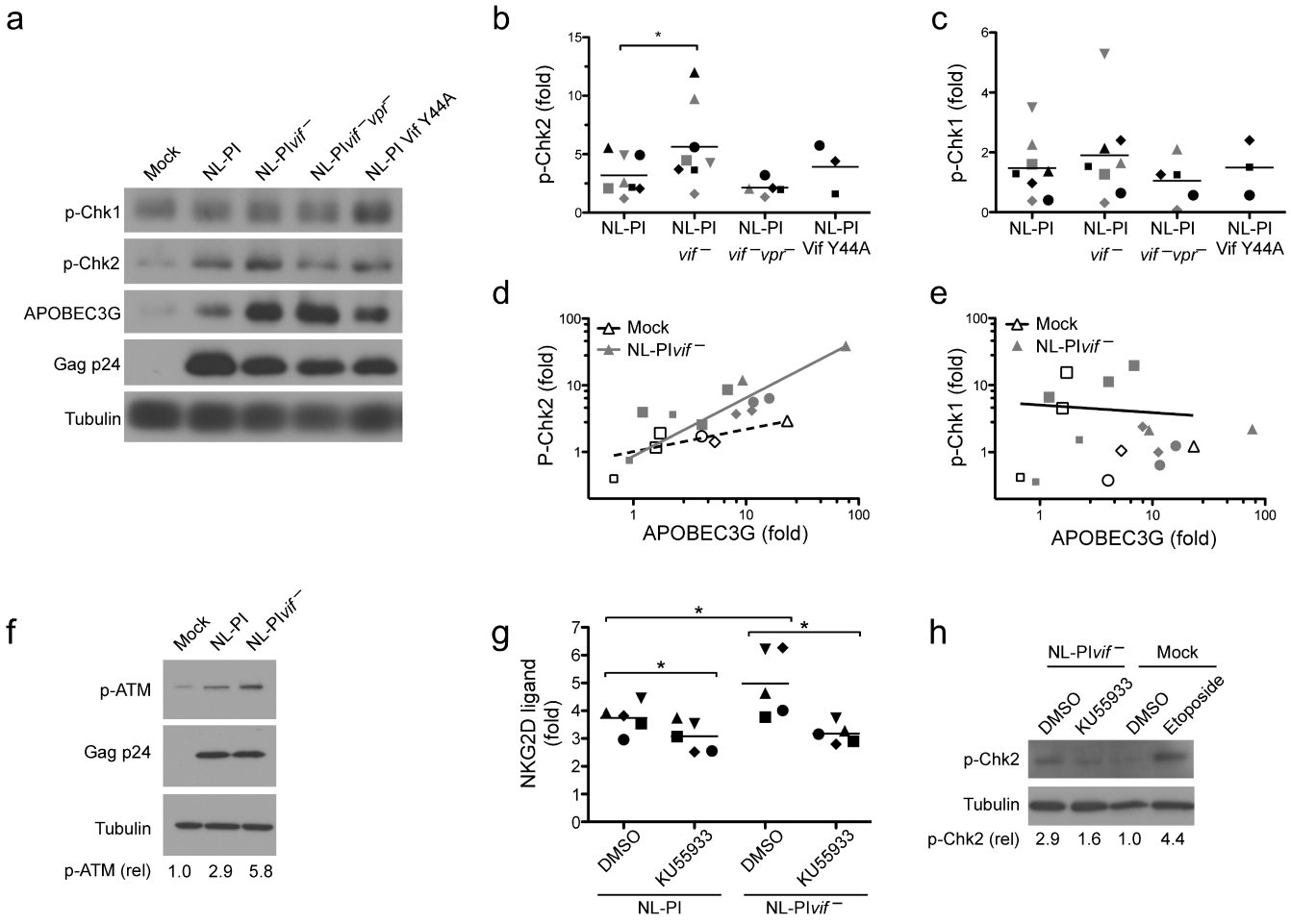

Figure 3. Activation of the DNA damage response in HIV infected primary T cells

(a) Representative immunoblot analysis of primary T cells infected with the indicated virus. **(b and c)** Summary plots of immunoblot analyses. **(b)** Chk2 phosphorylation at Thr_{68}; **(c)** Chk1 phosphorylation at Ser_{345}. Each independent donor is represented by a unique symbol. The black bar inidcates fold change relative to mock. **(d and e)** Relative A3G expression versus **(d)** Chk2 phosphorylation at Thr_{68} or **(e)** Chk1 phosphorylation at Ser_{345}. Each independent donor is represented by a unique symbol. Open symbols; mock infected plus conditioned supernatant. Gray symbols; infected plus or minus conditioned supernatant. For **(d)**, mock R^2=0.75, NL–PI*vif*$^-$ R^2=0.92, p<0.02. For (**e**), R^2=0.02. **(f)** Western blot analysis of primary T cells infected with the indicated virus measuring ATM phosphorylation at Ser_{1981}. **(g)** Summary plot of NKG2D ligand expression on primary T cells infected with the indicated viruses and treated with the ATM inhibitor KU55933 (10μM, Calbiochem) or solvent control. Data from five independent donors is shown. The black bars indicate the mean NKG2D ligand upregulation. Statistical analyses were performed by paired *t* test. * p<0.05 **(h)** Western blot analysis of primary T cells infected with NL-PI*vif*$^-$ and treated with KU55933 (10μM), solvent control or Etoposide (10μM, Sigma). Band intensities were quantified using Adobe Photoshop software, adjusted for background and normalized to α-

tubulin levels in the same lane. P-Chk2 expression relative to mock infected, solvent control is shown. Data are representative of three independent donors.

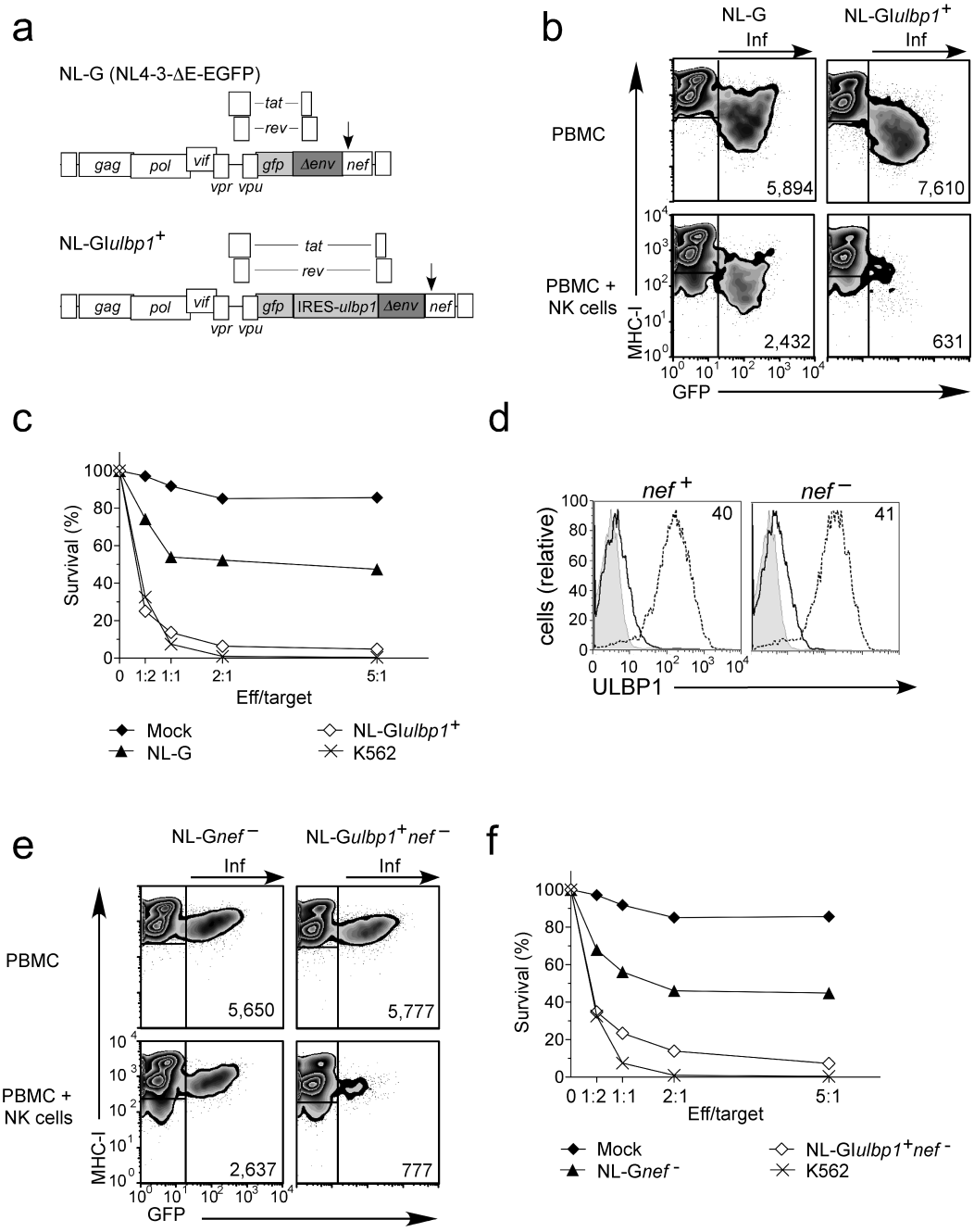

Figure 4. HIV–infected T cells are resistant to NK cell recognition unless an NKG2D ligand is overexpressed

(a) HIV genomes. NL4–3–ΔE–EGFP has been described[41]. Arrow indicates mutation in *nef*$^{-}$ construct. **(b)** Flow cytometric NK cell assay of primary T cells infected with the indicated virus and co–incubated with IL–2 stimulated autologous NK cells at a 2:1 effector to target ratio in a 4 hour cytotoxicity assay. Plots show MHC–I and GFP expression of 7–AAD^{-} CD56^{-} CD16^{-}, live target cells. Infected cells (Inf) are indicated. The total number of GFP^{+} cells normalized to counting beads is indicated. **(c)** Quantification of NK cell assay from

part **(b)**. The data are representative of three independent donors. The effector to target cell ratio (Eff/target) is indicated. **(d)** Flow cytometric analysis of ULBP1 expression in PHA-activated primary T cells transduced with NL–GI*ulbp1*$^{+}$, +/− *nef* (dotted black line) or NL–G +/− *nef* viruses (solid black line). ULBP1 expression of the transduced, GFP positive cells is shown. The solid gray histogram is the isotype control. The fold change in ULBP1 expression relative to control virus is indicated. **(e)** Flow cytometric NK cell assay of PHA activated primary T cells infected with the indicated viruses and co-incubated with autologous NK cells. 7–AAD^{-}CD56^{-}CD16^{-}GFP^{+} cells are shown and the number (normalized to counting beads) is indicated. **(f)** Quantification of NK cell assay from part e. The data are representative of two independent donors.

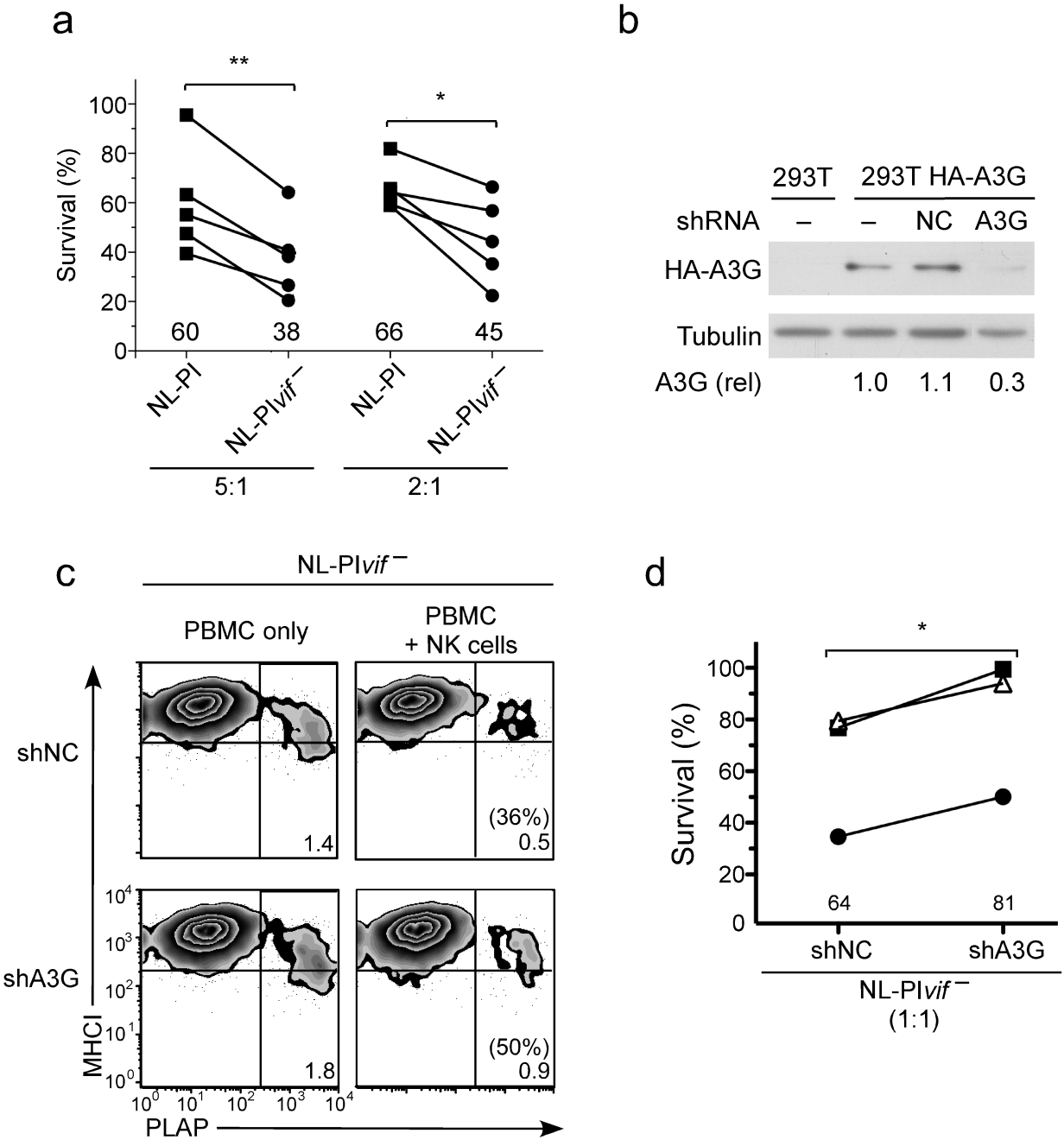

Figure 5. The effect of Vif on NK cell lysis

(a) Summary of flow cytometric NK cell killing assays from five independent donors. The percentage of infected cells surviving autologous NK cell treatment is shown. Mean T cell survival among the independent donors is indicated. * $p<0.05$, ** $p<0.01$. **(b)** Immunoblot analysis of 293T whole cell lysates transfected with the indicated shRNAs or untransfected (−). Band intensities were quantified using Adobe Photoshop software and normalized to tubulin expression. A3G expression relative to the untransfected control is shown. Data are representative of three experiments. **(c)** Flow cytometric NK cell assay of PHA activated

primary T cells infected with the indicated virus plus a GFP-expressing lentivirus encoding A3G–targeting or negative control shRNAs and co–incubated with IL–2 stimulated autologous NK cells at a 1:1 effector to target ratio in a 4 hour cytotoxicity assay. Plots show MHC–I and PLAP expression of GFP^+, 7–AAD^- $CD56^-$ $CD16^-$, live target cells. The percentage of infected cells with low MHC-I expression remaining after NK cell incubation is indicated. The percent cell survival with NK cells compared to without is shown in parentheses. **(d)** Summary of NK cell killing assay for three independent donors, indicated by different symbols. The mean cell survival at the indicated effector to target cell ratio (1:1) is indicated. In one of three experiments conditioned supernatant was required to observe an effect of A3G knockdown. Statistical analysis was calculated by paired *t* test. * $p<0.05$.

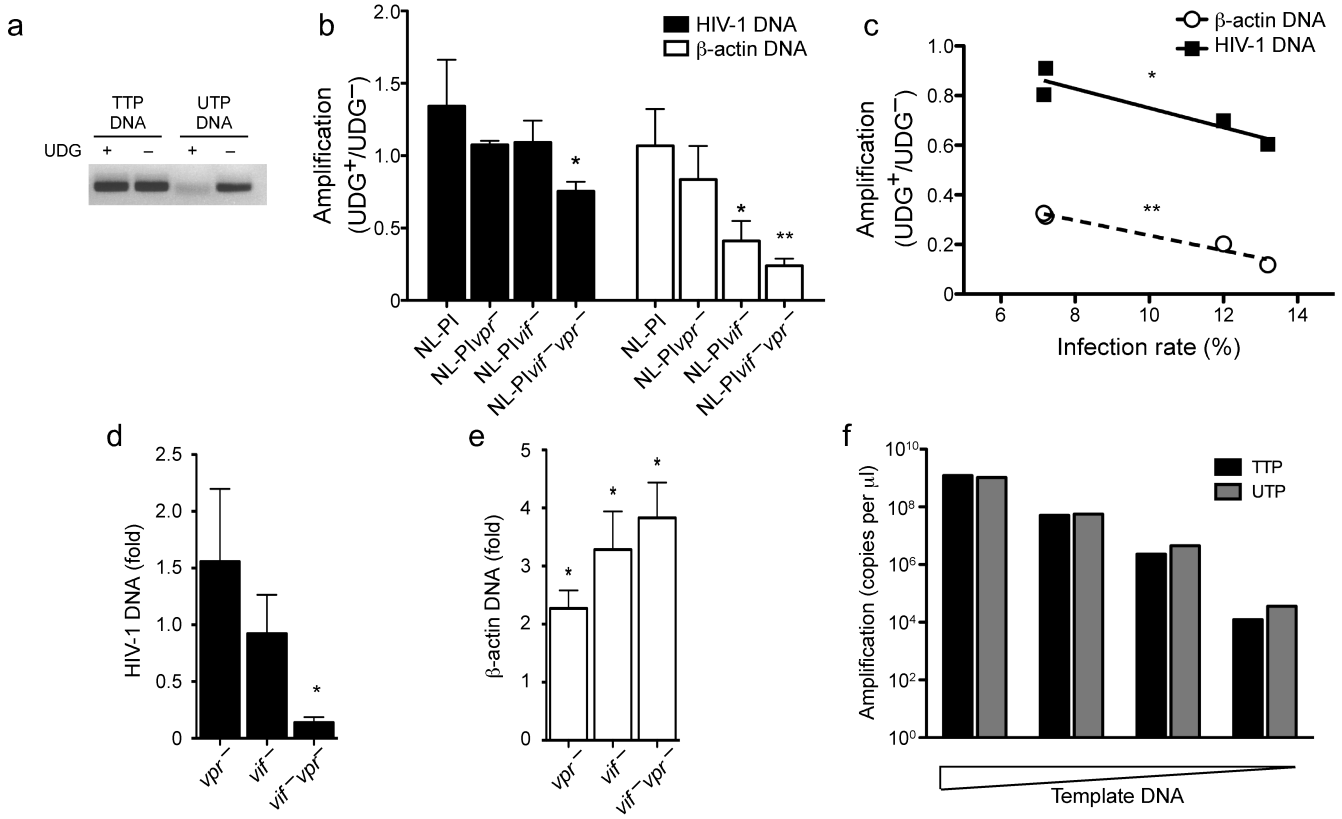

Figure 6. Vif and Vpr limit uridine incorporation in primary T cells

(a) Agarose gel of PCR products using NL-PI DNA containing dTTP or dUTP treated with recombinant UDG (+) or heat inactivated UDG (−) for 1 hour as template. **(b)** qPCR amplification results using total genomic DNA from primary T cells infected with NL-PI or the indicated virus mutant as template. DNAs were treated with UDG (+) or heat-inactivated UDG (−) prior to amplification. The graph shows the mean fold change in amplification with UDG^+ treatment from four independent donors. Statistical significance was determined by comparing to the theoretical mean of 1.0, which would represent no effect of UDG treatment. * $p<0.05$, ** $p<0.002$ **(c)** Graph of qPCR results from part **(b)** versus infection rate of NL-PI*vif* $^-$*vpr* $^-$ infected primary T cells. HIV-1 DNA; $R^2=0.86$, $p=0.07$. β-actin DNA; $R^2=0.96$, $p=0.02$. **(d and e)** qPCR amplification results of **(d)** total HIV DNA and **(e)** β-actin DNA isolated from primary T cells infected with the indicated viruses. In part **(d)** the mean was normalized for infection rate and β-actin DNA content. Standard error from four independent donors is shown. (d) * $p<0.002$, (e) * $p<0.05$ **(f)** qPCR amplification results of serially diluted NL-PI DNA templates containing dUTP or dTTP.

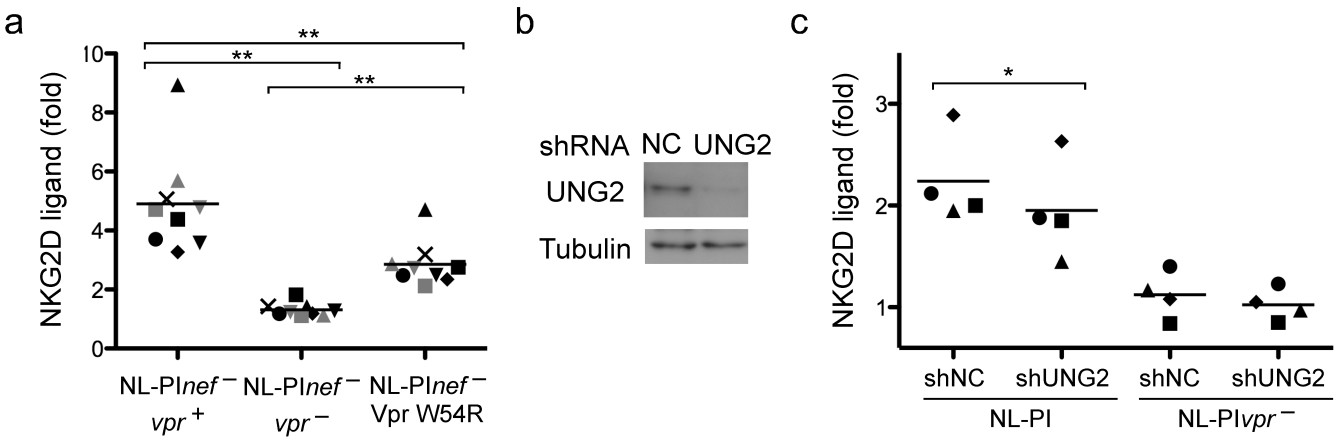

Figure 7. UNG2 binding by Vpr induces NKG2D ligand expression

(a and c) Summary plots of NKG2D ligand expression on activated primary T cells infected with the indicated viruses. The fold increase in NKG2D ligand expression relative to mock infected cells is shown. The mean expression for **(a)** eight and **(c)** four independent donors, indicated by different symbols, is represented by the black bars. Statistical analyses were performed by paired t test. * $p<0.05$, ** $p<0.01$. **(b)** Western blot analysis of CEM-SS T cells transduced with control or shUNG2-expressing lentivirus.